A stochastic sediment delivery model for a steep Mediterranean landscape

Emmanuel J. Gabet

Department of Geology, University of Montana, Missoula, Montana, USA

Thomas Dunne

Donald Bren School of Environmental Science and Management and Department of Geological Sciences, University of California, Santa Barbara, Santa Barbara, California, USA

Received 20 May 2003; accepted 17 June 2003; published 6 September 2003.

[1] It is a truism in geomorphology that climatic events operate on a landscape to drive sediment transport processes, yet few investigations have formally linked climate and terrain characteristics with geomorphological processes. In this study, we incorporate sediment transport equations derived from fieldwork into a computer model that predicts the delivery of sediment from hillslopes in a steep Mediterranean landscape near Santa Barbara, California. The sediment transport equations are driven by rainstorms and fires that are stochastically generated from probability distributions. The model is used to compare the rates and processes of sediment delivery under two vegetation types: coastal sage scrub and grasslands. Conversion of vegetation from sage to exotic grasses is a common land management strategy in the region and may also be engendered by regional climate change due to global warming. Results from the model suggest that (1) approximately 40% more sediment is delivered from grasslands (98 t km^{-2} yr^{-1}) than the sage scrub (71 t km^{-2} yr^{-1}) and (2) chronic soil creep processes dominate under grasslands whereas catastrophic processes dominate under coastal sage scrub. Results from the model also suggest that changes in the spatial distribution of vegetation arising from climate change will have a greater effect on sediment delivery than changes in the magnitude and frequency of meteorological events. *INDEX TERMS:* 1824 Hydrology: Geomorphology (1625); 1815 Hydrology: Erosion and sedimentation; 1803 Hydrology: Anthropogenic effects; 1869 Hydrology: Stochastic processes; *KEYWORDS:* geomorphology, landslides, erosion, fire, hillslopes, semiarid

Citation: Gabet, E. J., and T. Dunne, A stochastic sediment delivery model for a steep Mediterranean landscape, *Water Resour. Res.*, *39*(9), 1237, doi:10.1029/2003WR002341, 2003.

1. Introduction

1.1. Background

[2] With frequent fires, infrequent but intense rainfall, and sparse vegetative cover, the delivery of sediment from hillslopes in hilly Mediterranean landscapes is strongly episodic [*Rice*, 1982]. Whether sediment is delivered as a steady trickle or as large pulses can affect a wide range of geomorphic processes. For example, sediment delivery may come in the form of debris flows, which can cause significant property damage and the loss of life. Sediment production from hillslopes may overwhelm the transport capacity of the fluvial network and lead to flooding as well as the destruction of riverine habitats. Finally, over geological timescales, the frequency and magnitude of sediment delivery may control rates of bedrock incision [*Sklar and Dietrich*, 1998].

[3] In the absence of anthropogenic disturbances, climate ultimately determines the nature of sediment delivery. Climate regulates sediment production directly through meteorological events and, indirectly, by controlling the distribution of vegetation communities. For example, sediment transport by tree-throw contributes to soil creep in forested regions [*Denny and Goodlett*, 1956; *Gabet et al.*, 2003] but is not relevant in areas that are too dry for trees to grow. The influence of climate on the spatial pattern of vegetation communities, however, may be overridden by anthropogenic modifications. Indeed, in the Southwest United States, hillslopes are often cleared of brush and converted to grasslands. This conversion is usually done to increase forage for livestock [*Rice and Foggin*, 1971] but may also be done to reduce fire hazards and increase water yields [*Hibbert*, 1971]. A well-documented result of this land management strategy has been an increase in the frequency of landsliding on converted hillslopes [*Corbett and Rice*, 1966; *Bailey and Rice*, 1969; *Rice and Foggin*, 1971; *Terwilliger and Waldron*, 1991; *Gabet and Dunne*, 2002]. In light of predictions that under a warmer climate, the distribution of grasslands in California will increase at the expense of shrub communities [*Field et al.*, 1999], the effects of this management strategy may presage an underappreciated consequence of global climate change.

[4] A fundamental tenet in geomorphology holds that climatic events operating on a landscape drive sediment

0043-1397/03/2003WR002341$09.00

transport processes and hillslope evolution. *Rice* [1982] proposed a conceptual model that recognizes the stochastic nature of rainstorms and fires and their effects on shallow landslides, but, to date, few studies have formally (i.e., mathematically) linked climate and sediment transport. *Kirkby* [1976] applied a frequency distribution of daily rainfall to drive a process-based, hillslope hydrology model. With this model, he predicted annual runoff and related it to rates of sediment transport to model the evolution of hillslope profiles. *Dunne* [1991] demonstrated how variations in the frequency distributions of rainfall intensity and duration alter both the temporal pattern of sediment flux from hillslopes and the shape of hillslope profiles. *Dunne* [1991] also illustrated how the stochastic nature of climate is related to the spatial and temporal distribution of landsliding in the Pacific Northwest. *Benda and Dunne* [1997a, 1997b] furthered this approach with a process-based model of bedrock hollow-filling and landslide initiation. Their model combines random sequences of rainstorms and fires drawn from probability density functions (pdf's) with a landscape defined by a spatial distribution of characteristics (e.g., hillslope gradient, soil depth) also described by pdf's. *Iida* [1999] demonstrated the utility of rainfall pdf's for predicting the susceptibility of slopes to shallow landsliding. Finally, *Tucker and Bras* [2000] modeled the effects of rainfall variability on the evolution of drainage basins, illustrating that erosional thresholds can have morphological consequences.

[5] In this contribution, we expand upon the approach presented by *Benda and Dunne* [1997a, 1997b] and apply it to a hilly, semiarid watershed with a Mediterranean climate and two vegetation communities. The model proposed here includes all the dominant processes that we observed over a period of 5 years that encompassed a fire and the highest recorded annual rainfall in the region. The governing equations for the sediment transport processes have been developed and calibrated through fieldwork, and we assume that we have not overlooked any important process. With this model, we explore the effects of vegetation conversion and climate change on sediment production.

1.2. Field Area and Sediment Transport Processes

[6] The fieldwork and modeling efforts are centered on a hilly watershed in Sedgwick Reserve in the Santa Ynez Valley, near Santa Barbara, California (Figure 1). Located in the western portion of the Transverse Ranges, the field site is underlain by the Paso Robles Formation, a Pliestocene fanglomerate shed from the ancestral San Rafael Range [*Dibblee*, 1993]. The Paso Robles has been incised to produce gentle to steep rolling hillslopes with slope angles up to 45° and relief ranging from 30 to 50 m. The climate is Mediterranean with an average annual rainfall of 50 cm. The two main vegetation communities are coastal sage scrub (primarily *Artemisia californica* and *Salvia leucophylla*) and exotic grasses (various species of *Bromus* and *Avena*). Presently, grazing occurs on the grasslands at relatively low stocking rates (40 cow days ha^{-1} yr^{-1}).

[7] Few of the lower-order valleys at Sedgwick have channels, and there is approximately 1 m of fill in the first-order valleys. Little is known about the regional history, but presumably, the valleys began to fill with colluvium sometime after the region emerged from the latest glacial maximum, 16,500 years B.P. [*Kennett and Ingram*, 1995]. Under the drier conditions, the hillslope sediment delivery processes may have gained an advantage over the fluvial sediment transport processes. There is evidence that the channel network is beginning to expand after this phase of contraction. A knickpoint has been advancing up the main channel, Figueroa Creek, and tributary knickpoints are just beginning to form where the main knickpoint has moved past tributary valleys.

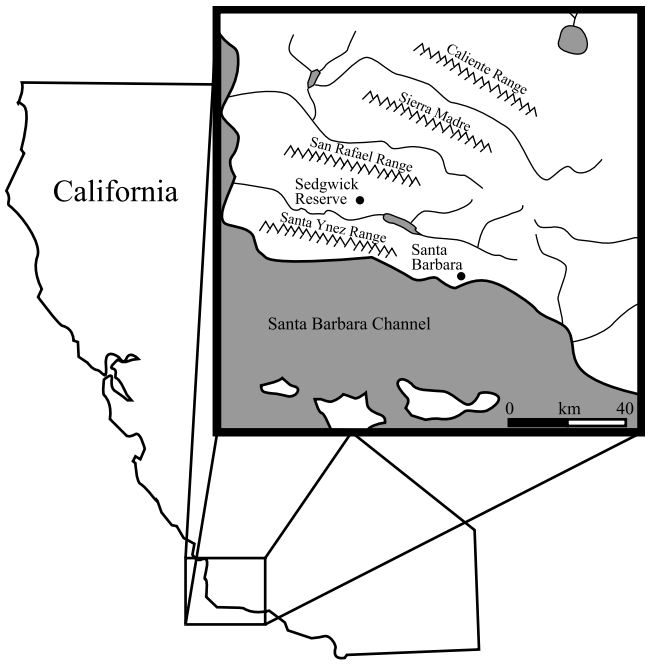

Figure 1. Site map for Sedgwick Reserve.

[8] Sediment is delivered to the valley bottoms at Sedgwick Reserve by three types of processes. The first, soil creep (*sensu lato*), includes bioturbation [*Gabet*, 2000] and dry ravel [*Gabet*, 2003b]. Second, sediment may be delivered by shallow landslides issuing from bedrock hollows [*Gabet and Dunne*, 2002]. Hollows accumulate sediment from adjacent hillslopes, and as the soil in a hollow thickens over time, it becomes increasingly susceptible to fail as a shallow landslide during heavy rainfall [*Campbell*, 1975; *Dietrich and Dunne*, 1978]. Fire may increase the likelihood of failure by destroying vegetation that increases soil strength through root cohesion. When a hollow is evacuated, it fills up again and the cycle repeats itself. The third important sediment delivery mechanism in this landscape is by thin debris flow (TDF) [*Wells*, 1987; *Gabet*, 2003a]. This process is limited to sage scrub vegetation and occurs when waxy organic molecules, vaporized during a fire from burning vegetation, recondense within the soil. This hydrophobic layer, deposited 1–2 cm below the soil surface, leads to a shallow perched water table during rainstorms. If pore pressures within this layer become sufficiently high, TDFs are triggered, stripping the top layer of soil [*Wells*, 1987; *Gabet*, 2003a]. Field observations indicate that the sediment flux from TDFs and the soil creep processes are not limited by the supply of sediment.

[9] Field observations and an extensive program of rainfall simulation experiments on plots that had undergone a variety of different treatments (i.e., trampled, burnt,

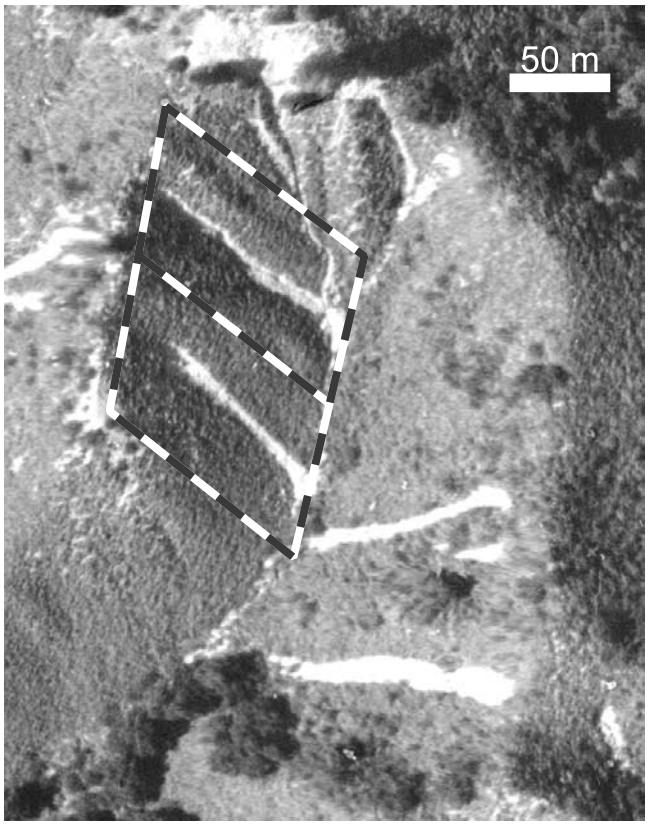

Figure 2. Aerial photo of a typical first-order valley at Sedgwick Reserve. The photograph was taken soon after a powerful El Niño-generated storm triggered more than 150 shallow landslides in the field area. In the coastal sage scrub, all of the landslides issued from bedrock hollows and mobilized as debris flows. The dashed lines demonstrate how the hillslopes may be represented as a series of rectangular strips, extending from one spur ridge to the next and encompassing a bedrock hollow.

mechanically denuded) suggest that overland flow does not appear to be an important transport process in either the sage or the grasslands. Infiltration capacities in the sage are sufficiently high to prevent the generation of Horton overland flow [*Fierer and Gabet*, 2002]. Even after a series of storms delivered rainfall to burnt hillslopes in the sage and triggered TDFs [*Gabet*, 2003a], there was no evidence of sediment transport by overland flow (e.g., the presence of rills or delta-like deposits of fine-grained material at the base of the slopes). In the grasslands, sediment transport by surface runoff is limited by the detachment of soil particles by raindrop impact [*Gabet and Dunne*, 2003]. Because the grazing pressure at Sedgwick Reserve is relatively light, the vegetation cover remains sufficiently high to shield the ground surface so that the annual sediment loss by overland flow is estimated to be 3–4 orders of magnitude less than by biogenic soil creep. This estimate is supported by observations made by the Sedgwick Reserve manager, who reported seeing clear water flowing down the hillslopes during intense rainfall (M. Williams, personal communication, 2001). Additionally, we did not observe any evidence of significant sediment transport from overland flow (e.g., rill formation or fine-grained deposits) on burnt grassland slopes.

2. Model Description

2.1. Model Domain

[10] A 2.1-km^2 watershed located in Sedgwick Reserve provides the topographic attributes for the model (Figure 2). In the model, the watershed is represented as a collection of 533 hillslope strips. Extending from the valley floor to the divide, hillslope strips are defined by three geometrical characteristics: length, width, and slope angle (Figure 3). Field observations and the U.S. Geological Survey (USGS) Los Olivos topographic map were used to measure the lengths and widths of hillslope strips where the width is defined as the distance between spur ridges that delimit the bedrock hollows. These measurements indicate that strip lengths and widths are normally distributed with means of 70 ± 10 m (1 standard deviation) and 35 ± 5 m (1 standard deviation), respectively. The distribution of slope angles was compiled from a digital elevation model (DEM) with 2-m spacing. The distribution of slope angles greater than 25° follows a Poisson distribution with a mean of 32° and a maximum of 45°. A minimum slope angle of 25° was chosen because it is a local threshold for TDFs [*Gabet*, 2003a] and debris flows mobilized from shallow landslides [*Gabet and Dunne*, 2002]. Additionally, 70% percent of the surface area of the modeled watershed is steeper than 25° so the flux from these hillslopes will dominate the total sediment delivered. Finally, a bedrock hollow, the source for shallow landslides, is ''embedded'' near the top of each strip (Figure 3). Figure 2 shows how this simple approximation of a rectangular strip with an embedded hollow may be appropriate for this landscape.

2.2. Climate

2.2.1. Rainstorms

[11] The climate is characterized as a series of rainstorms and fires. An annual sequence of rainstorms is determined

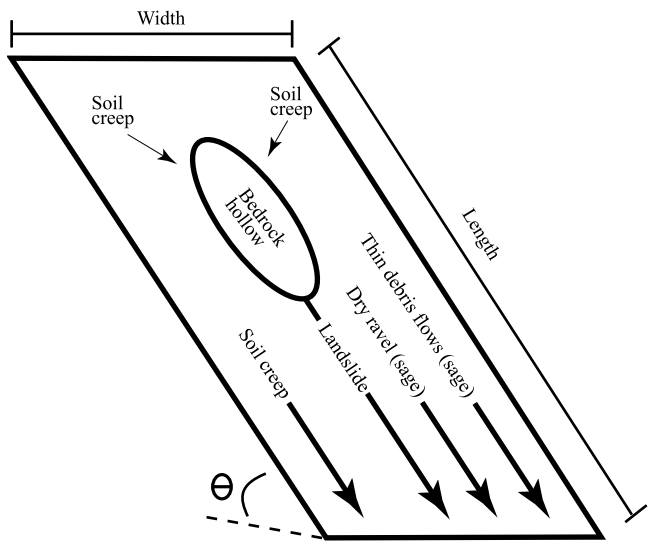

Figure 3. Hillslope strip. The modeled watershed is divided into 533 hillslopes strips, each with different topographic attributes. The potential transport processes operating on each strip are indicated.

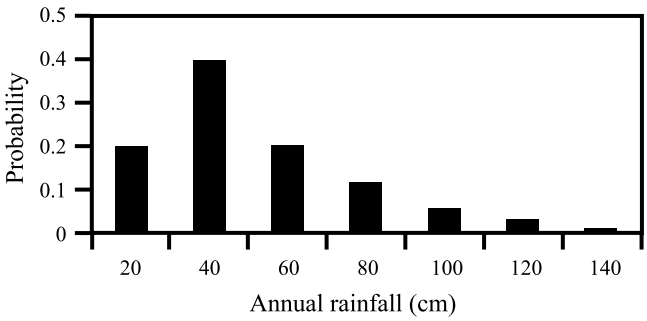

Figure 4. Probabilities of total annual rainfall. The data are from Cachuma Reservoir, 20 km southeast of Sedgwick Ranch.

by randomly selecting values from probability distributions for three variables. The first is total annual rainfall, and its probability distribution is based on 16 years of monthly rainfall records from nearby Cachuma Reservoir (Figure 4). The other two variables are storm duration and 1-hour precipitation intensity. These both follow independent exponential pdf's [*Eagleson*, 1972; *Beven*, 1987]:

$$P(i) = \left(\frac{1}{M_i}\right) e^{-i/M_i} \tag{1}$$

$$P(\tau) = \left(\frac{1}{M_\tau}\right) e^{-\tau/M_\tau} \tag{2}$$

where $P(\ )$ is the probability distribution function, i is 1-hour precipitation intensity (cm h^{-1}), and τ is storm duration (hours). Because only monthly rainfall totals were kept at Cachuma Reservoir, values for the mean intensity (M_i = 0.18 cm h^{-1}) and mean duration (M_τ = 14 hours) were determined from 12 years of hourly rainfall records from different local rain gauges (Buellton Fire Station and Figueroa Mountain Ranger Station; National Oceanic and Atmospheric Administration). The yearly sequence of storms is determined by randomly choosing an annual rainfall total from the pdf. Storm durations and intensities are then randomly chosen from their respective pdf's until the annual total is reached. The rainfall records in the area are relatively short, so we must make the assumption that they have captured a representative sample of the total population of rainstorms. It is encouraging to note that the hourly rainfall records include both the driest year and the wettest year recorded over the 16-year Cachuma Reservoir monthly data.

2.2.2. Fires

[12] Similar to the rainstorms, the generation of fires is also stochastic. Explicit fire models typically require input such as fuel load, wind direction, and topography [e.g., *Davis and Burrows*, 1993]. Rather than creating a complex fire submodel with data requirements beyond the scope of the sediment transport model, we have developed a stochastic approach that accurately produces the two critical characteristics of the fire regime: fire size distribution and average recurrence interval.

[13] The fire submodel has two components: fire ignition and fire propagation. Each cell in the model domain has a yearly ignition probability (I_p) determined with

$$I_p = B_p(1 - e^{gt_f}) \tag{3}$$

where B_p is base ignition probability, g is a vegetation growth constant (yr^{-1}), and t_f is time since the last fire (years).

[14] According to this function, the ignition probability increases as vegetation regrows after a fire, asymptotically approaching a maximum as the plant matures (values for g are discussed later with equation (9b)). At the yearly time step, a random number is chosen for each cell and compared to I_p. Any cell that has a random number smaller than I_p becomes the locus for a fire. When a fire is ignited, another random number is selected and compared to a probability distribution of fire sizes. The distribution of fire sizes in the region may be approximated by a negative exponential function (J. Keeley, U.S. Geological Survey, personal communication, 2000)

$$P(F) = \left(\frac{1}{M_F}\right) e^{-F/M_F} \tag{4}$$

where F is fire size (ha) and M_F is mean fire size. The fire propagates radially from the ignited cell into neighboring cells until the chosen size is attained. After a cell is burned, t_f is reset to zero. Over time, the landscape becomes a mosaic of vegetation of different age classes (Figure 5). It

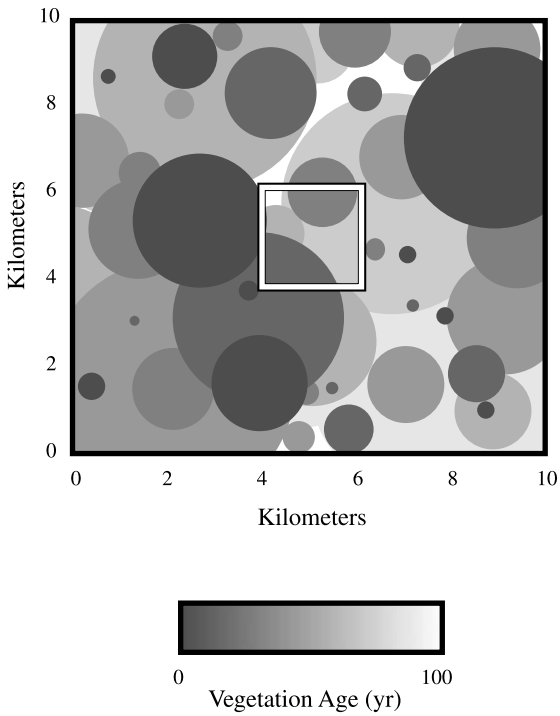

Figure 5. Distribution of vegetation ages in model domain. Vegetation age at any cell is an indicator of the time since the previous fire. To avoid edge effects, the sediment transport model domain (outlined in white box) occupies a small area (2.1 km^2) in the middle of the larger fire submodel (100 km^2).

might be argued that propagation of the fire should be dependent on vegetation age; however, *Keeley et al.* [1999] concluded that brushland fires burn equally well through all age classes. It might also be argued that fires rarely propagate radially from an ignition point. This simplification, however, may be appropriate because we are interested in understanding the temporal pattern of sediment loading rather than the spatial distribution of sediment delivery to a topologically defined channel network. Therefore the average fire recurrence interval on a hillslope is more important than the particular location of a burnt hillslope.

[15] This fire submodel depends on only two variables, the base ignition probability and the mean fire size. *Keeley et al.* [1999] report that the pre-1951 mean brush fire size for Santa Barbara County is 1622 ha and 2341 ha after 1951; however, these averages are higher than the true average because small fires are often not recorded by government agencies [*Keeley et al.*, 1999]. Nonetheless, by assuming a negative exponential distribution of fire sizes, the frequency of fires >100 ha presented by *Keeley et al.* [1999] can be used to reconstruct the entire distribution of fire sizes to yield a post-1950 mean fire size of 650 ha.

[16] The base ignition probability, in contrast, is determined by inverse modeling. *Keeley et al.* [1999] report a post-1950 fire rotation interval of 81 years. Because the fire rotation interval is equal to the average vegetation age [*Wagner*, 1978], the base ignition probability can be determined iteratively. An initial B_p is chosen and the model is run until the average vegetation age for the entire model domain becomes approximately constant. This average age is then compared to the desired fire rotation interval and B_p is adjusted until they match.

[17] We are not aware of any data on fire size and recurrence interval for grassland fires for the region, so we use the same fire parameters for the grasslands as for the coastal sage scrub. The effects of this limitation are minimal because of the relative insensitivity of the grassland transport processes to fire. First, there was no evidence of soil hydrophobicity, increased runoff rates, or rill formation in burnt grasslands after a fire on the property adjacent to Sedgwick Reserve. Second, grass regrows after the first rains of the winter season so that any loss of root strength that would increase the likelihood of shallow landslides would be minor. Finally, the rapid regrowth of grass would quickly shield the bare soil from raindrop impact.

2.3. Infiltration

[18] One of the first-order controls on hillslope sediment transport processes is the partitioning of rainfall between surface and subsurface flow. Average values for the infiltration capacity, 14 cm h^{-1} for sage and 0.5 cm h^{-1} for grassland, were measured with a rainfall simulator [*Fierer and Gabet*, 2002; *Gabet and Dunne*, 2003]. The creation of a hydrophobic layer in the sage scrub soil during a fire, however, can reduce infiltration capacities [*DeBano*, 1981]. A study by *Cerda* [1998] in eastern Spain indicates that recovery of the prefire infiltration capacity occurs within 4–5 years in Mediterranean shrubland. Although the vegetation community in *Cerda*'s [1998] study differs from the vegetation in this study, we are interested in the rate of decay of hydrophobicity, rather than the absolute values of infiltration capacity. Assuming that temporal changes in soil hydrophobicity in coastal sage are similar to chaparral, *Cerda*'s [1998] data indicate that changes in infiltration capacity (f; cm h^{-1}) at the yearly time step can be calculated as follows:

$$f(t) = f_i + (f_f - f_i)e^{-kt_f} \tag{5}$$

where f_i is prefire infiltration capacity, f_f is infiltration capacity immediately after the fire, and k is a constant (year^{-1}).

[19] On the basis of *Cerda*'s data [1998], k varies between 0.7 and 1.2, and we use an intermediate value of 1. From *Gabet* [2003a], f_f is taken to be 0 cm h^{-1} at a depth 1.5 cm below the surface of the soil.

2.4. Soil Creep

[20] The flux from slope-dependent soil creep processes is calculated as an average annual rate and is independent of rainstorms and fires. Soil creep in the sage is primarily by dry ravel, the downslope movement of individual particles by rolling, sliding, and bouncing. The annual specific mass flux by this process (i.e., flux per unit contour width of hillslope), q_s (kg m^{-1} yr^{-1}), is determined with [*Gabet*, 2003b]

$$q_s = \frac{\kappa}{\mu\cos\theta - \sin\theta} \tag{6}$$

where κ is 0.056 kg m^{-1} yr^{-1} and μ is 1.01. The value given here for the coefficient of kinetic friction, μ, is greater than the one inferred from sediment trap data by *Gabet* [2003b]. Vegetation density and lithology vary slightly throughout Sedgwick Reserve, and therefore the friction coefficient may differ from one hillslope to the next. For consistency, we set μ just higher than 1.0, the steepest gradient for soil-mantled hillslopes at Sedgwick Reserve. Because of the highly nonlinear nature of equation (6), we would prefer to assign μ values to individual hillslope strips from a pdf; however, we do not have sufficient field data to determine the spatial frequency of μ.

[21] The dominant creep process in the grasslands appears to be bioturbation by pocket gophers, and its specific mass flux is calculated as a function of slope with [*Gabet*, 2000]

$$q_s = \frac{19(\tan\theta)^3 - 20.4(\tan\theta)^2 + 7.3(\tan\theta) + 3.7(\tan\theta)^{0.4}}{\cos\theta} \tag{7}$$

The above equation is divided by cosθ to account for the total flux, rather than just the horizontal component of flux as presented by *Gabet* [2000].

2.5. Shallow Landslides

[22] A stability analysis is performed at every yearly time step on each bedrock hollow to determine whether a shallow landslide is triggered. *Reistenberg and Sovonick-Dunford* [1983] and *Gabet and Dunne* [2002] demonstrated that the commonly used infinite-slope stability analysis [e.g., *Selby*, 1993] needs to be expanded when lateral root reinforcement is important. Neither the roots of coastal sage nor grass penetrate the bedrock, and therefore the root reinforcement on the modeled hillslopes is entirely in the lateral direction. To account for lateral root reinforcement,

we use the stability analysis derived by *Gabet and Dunne* [2002] where the factor of safety (S) is calculated with

$$S = \frac{C'_{rl}\left(\frac{2z_{rd}\cos\theta}{\sin\alpha}\right) + C_s\left(w + \frac{2z\cos\theta}{\sin\alpha}\right) + wz(\gamma_s - m\gamma_w)\cos^2\theta\tan\phi}{wz\gamma_s\cos\theta\sin\theta} \quad (8)$$

where

C'_{rl} effective lateral root cohesion (kPa);
C_s soil cohesion (kPa);
m fraction of the soil column that is saturated;
w failure width (m);
z failure depth (m);
z_{rd} rooting depth (m);
α side-scarp angle (deg);
ϕ internal angle of friction (deg);
γ_s unit weight of wet soil (kN m^{-3});
γ_w unit weight of water (kN m^{-3});
θ hillslope angle (deg).

Values for the constants above are summarized in Table 1.

[23] The lateral root reinforcement (the first term on the left-hand side of equation (8)) depends on the rooting depth and the lateral root cohesion. Root cohesion can vary in time because of plant death and regrowth. To simulate root decay and regrowth after a fire, the effective lateral root cohesion (C'_{rl}) is calculated with

$$C'_{rl} = C_{rl}(G + D) \quad (9a)$$

$$G = 1 - e^{-gt_f} \quad (9b)$$

$$D = e^{-dt_f^n} \quad (9c)$$

$$G + D \leq 1 \quad (9d)$$

where

C_{rl} maximum lateral root cohesion (kPa);
D root decay factor;
G root growth factor;
d, n root decay constants;
g vegetation growth constant;

the same as in equation (3). Following *Sidle* [1992], the decay of root cohesion is represented by an exponential function (9c). However, whereas *Sidle* [1992] suggests the use of a sigmoid function for the growth curve, we choose a simpler function (9b) that reflects the dearth of appropriate data for coastal sage scrub vegetation. The root growth curve is calibrated to aboveground growth data for sage vegetation [*Horton and Kraebel*, 1955], yielding a value of 0.15 for g. No published data exist for d and n for coastal sage, so they must be estimated indirectly. Some types of vegetation in Mediterranean ecosystems resprout after fires, and therefore root decay would be minimal. However, the dominant species at Sedgwick, California, sagebrush and black sage, typically are not resprouters [*Horton and Kraebel*, 1955; *Keeley*, 1986]. As a starting point for estimating values for d and n, there is a 90% decrease in root strength 8 years after death for Douglas fire [*Burroughs and Thomas*, 1977]. If we assume that sage roots experience a 90% decrease in strength after 4 years, values for d and n would be 0.8 and 0.7, respectively. It is simpler to estimate the constants (g, d, n) for the grass because grass will grow back immediately after a fire with the onset of rains and the fine grass roots likely decay quickly as well. Therefore, to simulate these rapid response times, g is 3, d is 2.8, and n is 0.7, such that both root growth and root decay reach 95% of their maximum after 1 year. Finally, the value for C_{rl} is 1 kPa for grass and 3 kPa for sage [*Terwilliger and Waldron*, 1991].

Table 1. Values for Constants in Stability Analysis

Constant	Value
C_s	1.2 kPa
z_{rd} (grass)	0.15 m
z_{rd} (sage)	1.00 m
α	45°
ϕ	32°
γ_S	13.9 kN m^{-3}
γ_w	9.8 kN m^{-3}

[24] Whereas root strengths determine the vulnerability of soils to failure, it is the rise in pore pressure during storms that triggers the landslides, and therefore the degree of saturation (m) in the bedrock hollows must be determined for the stability analysis. Following *Dunne* [1991] and *Benda and Dunne* [1997b], the convergent bedrock topography into a hollow is idealized as a conical depression. The peak saturated soil thickness (H) at any point x along a horizontal radius can be calculated with

$$H = I_e x(r - 0.5x)/K\sin\theta(r - x) \text{ if } x < x_s \quad (10a)$$

$$H = I_e x_s(r - 0.5x_s)/K\sin\theta(r - x) \text{ if } x > x_s \quad (10b)$$

$$x_s = K\sin\theta\cos\theta T/p \quad (10c)$$

where x_s is the downslope distance beyond which subsurface flow attains steady state. I_e is the average effective rainfall intensity (mm h^{-1}) for a storm of duration T, and only the largest storm of the model year is considered [*Benda and Dunne*, 1997b]. The effective rainfall intensity reflects the limits imposed by the infiltration capacity to properly account for the effects of soil hydrophobicity after a fire. From field measurements, the average saturated hydraulic conductivity (K) is 0.65 m h^{-1} and the colluvium's drainable porosity (p) is 0.2 (O. Chadwick, University of California, Santa Barbara, personal communication, 2001). The radius of the cone, r, is 50 m, an average from measurements of hollows at Sedgwick Reserve. Again, following *Benda and Dunne* [1997b], pore pressures are not calculated at every horizontal radial distance x [*Dunne*, 1991]. Instead, the pore pressure is calculated at 15 m, a radial distance included in most of the failures observed at Sedgwick Reserve. With the value for H determined with (10), m in equation (8) is calculated with

$$m = \frac{H}{z\cos\theta} \quad (11)$$

[25] Surveys of the failures at Sedgwick Reserve revealed a systematic decline in failure width with increasing slope in the sage [*Gabet and Dunne*, 2002]. From the data presented by *Gabet and Dunne* [2002], failure width in equation (8) is calculated as a function of slope with

$$w = 12(\theta - 31)^{-0.5} \tag{12}$$

For slopes less than 32°, failure widths are set at 13 m. Because there was no apparent relationship between failure width and slope in the grasslands, the average width for grassland failures (5 m) is used [*Gabet and Dunne*, 2002]. Failure volumes are determined as the product of the width, the soil depth at failure, and the failure length calculated from the average length/width ratio (2.7) [*Gabet and Dunne*, 2002].

2.6. Hollow Filling

[26] After a bedrock hollow is evacuated, the landslide scar is refilled by sediment transported from adjacent slopes by soil creep. The net volume (V) of sediment coming into the hollow per meter length of scar (l) can be calculated as a function of time since the previous landslide (t_l) with

$$\frac{V(t_l)}{l} = \frac{2q_s t_l \sin\lambda}{\rho_s} \tag{13}$$

where ρ_s is the dry bulk density of the soil and λ is the convergence angle into the hollow [*Reneau and Dietrich*, 1991]. Landslide scars are represented as troughs with side-scarps at an angle α [*Gabet and Dunne*, 2002] such that the soil depth in each hollow (z) can be expressed as a function of time since the previous landslide with [*Benda and Dunne*, 1997b]:

$$z(t_l) = \left[\left(w^2 + 4V(t_l)\cot\alpha\right)^{0.5} - w\right]\frac{\tan\alpha}{2} \tag{14}$$

Average values from Sedgwick Reserve for ρ_S and λ are 1190 kg m^{-3} and 32°, respectively.

2.7. Postfire Transport Processes

[27] In addition to background dry ravel, there is a form of dry ravel associated with fire. In steep semiarid environments with shrubby vegetation, transport by dry ravel after a fire can be extensive, as sediment that has accumulated behind litter and vegetation is released when the vegetation is burned [*Wells*, 1987; *Florsheim et al.*, 1991]. From sediment traps installed in coastal sage scrub in anticipation of a prescribed fire near Sedgwick Reserve, the specific flux of sediment from postfire dry ravel can be determined with equation (6) with a value of 0.03 kg m^{-1} fire^{-1} for κ and 1.01 for μ. The amount of postfire dry ravel reported here is less than what has been observed elsewhere. For example, *Wells* [1987] observed that small channels in the San Dimas Experimental Forest, near Los Angeles, were completely filled with dry ravel deposits immediately after a fire in shrubby vegetation. *Davis et al.* [1989] found that 0.20 m^3 of dry ravel deposits were delivered per meter length of channel in the month following a chaparral fire near Santa Barbara. Assuming a bulk density of 1300 kg m^{-3} for the deposit and assuming that the deposits accumulated from both sides of the channel, the specific mass flux was then 130 kg m^{-1}. This is significantly more than what was observed near Sedgwick Reserve; for example, equation (6) parameterized with the values for κ and μ above predicts a specific mass flux of 0.20 kg m^{-1}. A difference in lithology is the most likely explanation for the discordance between the rates of postfire dry ravel at Sedgwick Reserve and those reported by *Davis et al.* [1989]. The watershed studied by *Davis et al.* [1989] is underlain by shale and sandstone and the clasts in the postfire dry ravel deposits were well sorted, with an average size of 4 mm [*Florsheim et al.*, 1991]. In contrast, the fanglomerate at Sedgwick Reserve weathers into particle sizes that range from clay to gravel. A greater variance in particle size will decrease the flux by increasing the effective roughness of the surface [*Kirkby and Statham*, 1974]. Additionally, the soils at Sedgwick Reserve are generally high in smectitic clays [*Shipman*, 1972], and the cohesion from these clays may inhibit raveling.

[28] Along with dry ravel, thin debris flows (TDFs) are also limited to the coastal sage scrub. *Gabet* [2003a] has developed a numerical model for TDFs that couples subsurface flow routing through the top 1–2 cm of soil with an infinite-slope stability analysis. The TDF model predicts the location and timing of these shallow failures during rainstorms such that the mass of sediment transported across a unit contour width of slope by TDF may be determined with [*Gabet*, 2003a]

$$\frac{\text{mass}}{\text{unit width}} = ALz_t\rho_{st} \tag{15}$$

where

A fraction of area covered by TDF scars;
L length of TDF scar (m);
z_t failure depth (m);
ρ_{st} bulk density of the top layer of soil (kg m^{-3}).

L is determined with the model described above; from field observations, d is 1.5 cm and A is 0.60 [*Gabet*, 2003a]. The bulk density of the upper layer of soil, adjusted for organic content, is 560 kg m^{-3} [*Gabet*, 2003a].

[29] Many simulation runs of the TDF model described by *Gabet* [2003a] were done to determine the excess rainfall (i.e., $i - f$) thresholds necessary for triggering TDFs at various slope angles. These runs indicated that only about 0.3 cm of rain will cause TDFs, which agrees well with *Wells* [1987]. In the larger model presented here, when the rainfall threshold is reached, the sediment delivered to the base of the hillslope is determined with equation (15).

2.8. Model Operation

[30] The algorithm for the model is shown in Figure 6. The climate parameters, mean rainfall intensity, mean storm duration, mean fire size, and fire recurrence interval are specified at the beginning of each run and can be changed at any time during the run. Similarly, vegetation type, which determines the suite of relevant transport processes, is specified for each hillslope strip at the start of the model simulation and can be changed at any time. The initial soil depth in each bedrock hollow is determined by randomly assigning a value for t_l, the time since the last landslide (see equations (13) and (14)). Values for t_l are normally distributed with a mean of 100 years such that initial soil depths are less than 0.20 m. Because slope angles and soil depths

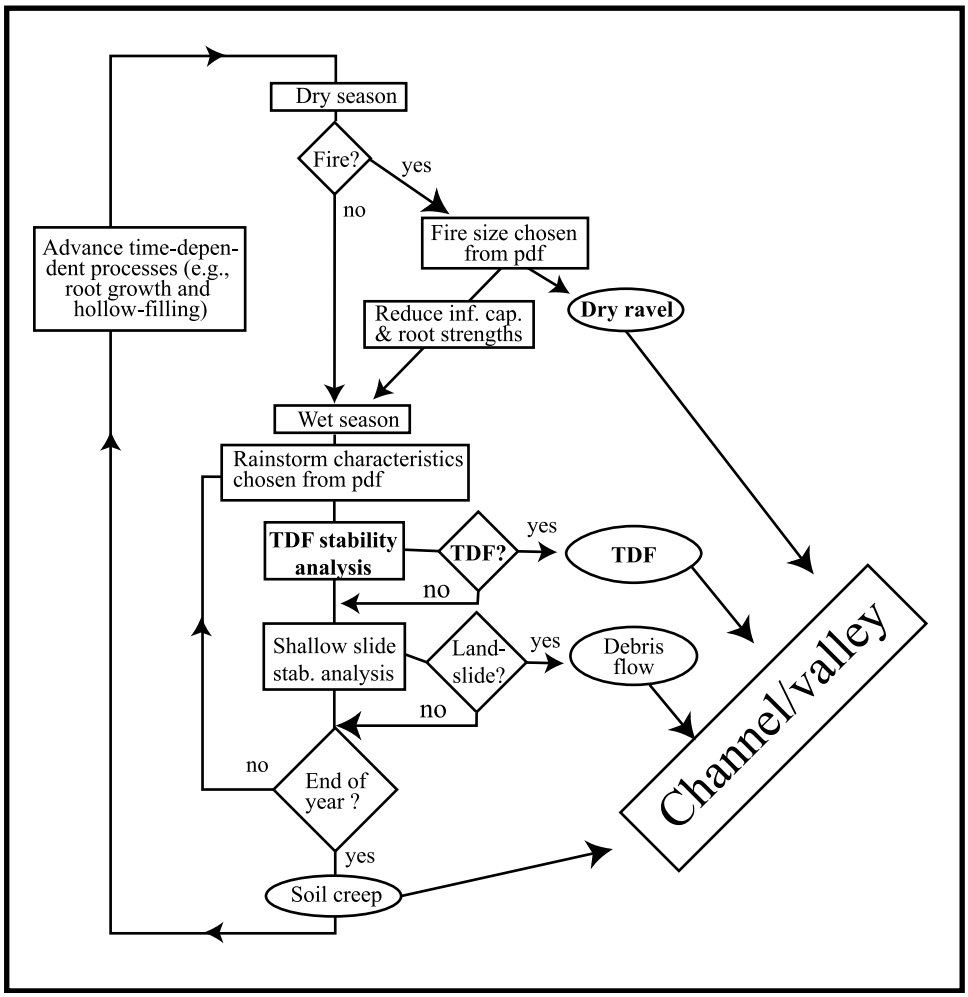

Figure 6. Algorithm for the sediment delivery model. Ovals represent sediment transport processes. Processes in bold type occur only in the coastal sage scrub.

(via t_l) are independently chosen from pdf's, there is a risk that a number of hollows will be initially unstable and fail immediately once the model runs begin. Initial depths therefore are low to avoid artificially synchronizing the cycle of filling and failing among the hollows. To further reduce the effect of the initial conditions, each simulation is run for 5000 years before the results are considered.

[31] To summarize the spatial parameterization of the model, Figure 3 illustrates the geometrical properties of an individual hillslope strip and the transport processes that deliver sediment to the channel network. An example of the sediment output for an individual strip vegetated by coastal sage is shown in Figure 7. For the first 8 years, the only sediment comes from soil creep. In the eighth year, there is a fire on the strip, causing a pulse of sediment from dry ravel and TDFs. Because of the hydrophobic layer and the lag in the root strength loss, there is no landslide in that year. The following year, however, the combination of high rainfall and loss of root strength leads to the evacuation of the bedrock hollow.

[32] At the watershed scale, the processes described above are repeated for all 533 strips. The model records the annual amount of sediment delivered to the base of each hillslope but does not route the sediment down the channel network. Watersheds in California have valley floors in various stages of aggradation and degradation, and therefore the fate of sediment once it reaches the base of the hillslope is dependent on processes beyond the scope of this model.

3. Results and Discussion

3.1. Model Test

[33] The main high-resolution prediction of the model, a time series of sediment production, cannot be tested because there are no long-term records of sediment discharge from Sedgwick Reserve. However, results from the model can be used to predict an average rate of sediment delivery that can be compared to a rate determined from a sedimentation survey at nearby Gibraltar Reservoir (approximately 40 km southeast of Sedgwick Reserve). In contrast to Sedgwick Reserve, active channels are connected to the base of the hillslopes and there is little storage of colluvium on the footslopes. This tight linkage between the hillslopes and the fluvial network suggests that averaged over several years, the sediment yield from the Gibraltar watershed may be equivalent to the total amount of sediment produced from the hillslopes.

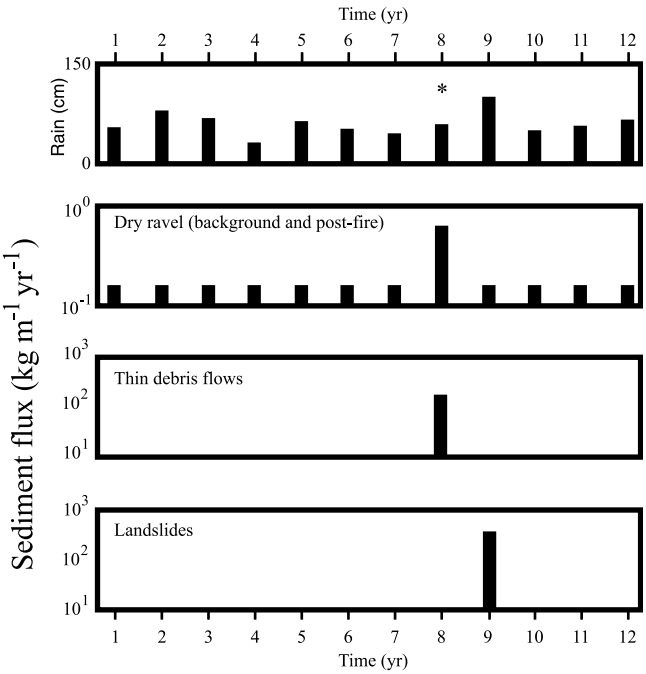

Figure 7. Illustration of the sediment delivery from one hillslope strip with sage vegetation. The top panel is the annual rainfall with a fire in the eighth year indicated by an asterisk. The second panel is the sediment flux from dry ravel and includes both the background rate and the pulse of dry ravel after a fire. The third panel represents the sediment delivered from TDFs during rainstorms after the fire. The bottom panel is the delivery of sediment from a shallow landslide.

[34] The watershed upstream of the Gibraltar Reservoir is steeper than the one modeled at Sedgwick Reserve so the topographic attributes must be redefined. From an analysis of the USGS Little Pine Mountain quadrangle, the average hillslope length is approximately 110 m and the average slope angle is 36°. With these hillslope parameters and a coastal sage scrub vegetation cover, the model predicts an average sediment yield of 128 t km^{-2} yr^{-1}. Data from the Santa Barbara County Water Agency (SBCWA) indicate that averaged over 25 years, the volumetric sediment yield from the Gibraltar Reservoir watershed is approximately 640 m^3 km^{-2} yr^{-1}. Although the bulk density of the sediment has not been measured (K. Goodenough, SBCWA, personal communication, 2001), bulk densities for fine-grained reservoir deposits may vary from 370 to 530 kg m^{-3} [*Meade*, 1966]. With these values, the mass sediment yield into Gibraltar Reservoir is 250–360 t km^{-2} yr^{-1}.

[35] The predicted rate is 25% less than the lowest rate estimated from the reservoir data. It is possible that we have overlooked an important transport process; however, the difference between the model results and the calculated sediment yield is likely to due to an underprediction in the rates of dry ravel. As previously noted, the soils at Sedgwick Reserve do not appear to be as susceptible to dry ravel as coarser soils. In contrast, the lithology of the Gibraltar Reservoir watershed is dominated by shales and sandstones, similar to the bedrock that produced the high rates of postfire dry ravel measured by *Davis et al.* [1989]. To approximately match *Davis et al.*'s [1989] data, the value of κ is increased to 33 kg m^{-1} $fire^{-1}$ in equation (5). Additionally, data reported by *Anderson et al.* [1959] and *Krammes* [1965] from the San Gabriel Mountains in southern California may be used to estimate a value of 2.5 kg m^{-1} yr^{-1} for background dry ravel. The San Gabriel Mountains are granitic, producing sand-sized weathered material [*Anderson et al.*, 1959], similar to the regolith in the Gibraltar watershed. With these new values, the predicted yield becomes 346 t km^{-2} yr^{-1}, suggesting that the model is capturing the essence of sediment delivery in this type of landscape. Ideally, we would have used a detailed fire and precipitation record from the Gibraltar watershed to drive the model; unfortunately none exist. However, the watershed may be large enough (520 km^2) that it may integrate the range of climatic events represented in the model run. Additionally, surveys from other reservoirs in the region (Juncal, Twitchell, and Bradbury) record sediment yields similar to the Gibraltar watershed (SBCWA).

3.2. Vegetation Change at Sedgwick Reserve

[36] As previously noted, human-induced vegetation conversion from native scrub to exotic grasses is a common practice in the region. Additionally, coupled climate-vegetation models predict that in the next 100 years, grassy savanna communities may replace shrublands throughout the Coast Ranges of California [*Field et al.*, 1999]. To investigate the effects of vegetation change on sediment delivery, the model was run under sage for 10,000 years and then run under grasslands for another 10,000 years. Ten thousand years was chosen because the model runs must be long enough such that differences resulting from changes in the model parameters can be distinguished from variations caused by the stochastic forcing.

[37] From Figures 8 and 9, there are noticeable differences in sediment delivery between the sage and the grasslands. In the coastal sage scrub, there is greater interannual variability in annual sediment delivery, whereas in the grasslands, sediment delivery events are relatively muted. Figure 9 also shows that the rate of soil creep is approximately 4 times greater in the grasslands than in the coastal sage. Average rates of annual sediment delivery and spatially averaged soil erosion rates for both vegetation types are listed in Table 2. These results suggest that sediment delivery is 38% higher under grassland than coastal sage.

[38] The primary reason for the marked difference in the nature of sediment delivery between the two vegetation covers is attributable to the difference in relevant transport processes. The relative magnitudes of the different processes are compared in Figure 10. In the sage, 70% of the total sediment delivered is by catastrophic processes: TDFs and landslides. This indicates that sediment delivery in the sage is strongly linked to the occurrence of fires. In contrast, soil creep accounts for 72% of the sediment production in the grasslands. Because of the absence of TDFs in the grasslands, sediment production is not as sensitive to fires. Therefore vegetation conversion changes not only the magnitude of sediment supply but also the nature of sediment delivery from catastrophic to chronic. Finally, the relatively weak contribution of grass roots to overall soil strength, as well as its rapid regrowth after a fire, decouples the occurrence of landslides from the fire regime.

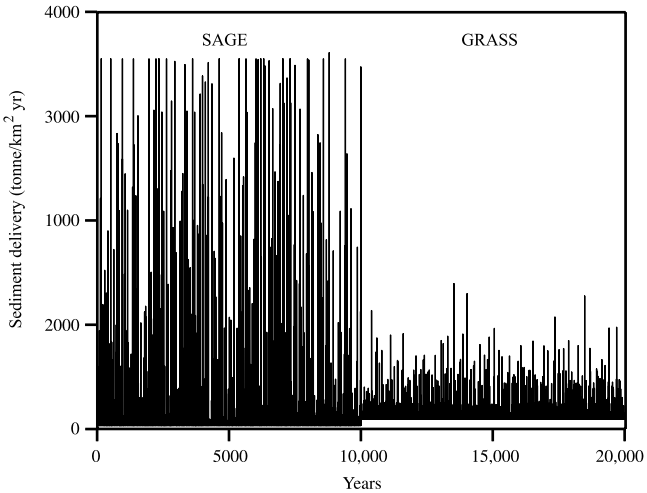

Figure 8. Predicted annual sediment delivery with vegetation conversion. The first 10,000 years are with sage vegetation and the last 10,000 years with grass. The amount of sediment delivered each year in the sage has a higher interannual variability than in the grasslands (note that the maximum sediment delivery occurs in the coastal sage each time the entire model domain burns). In the grasslands, the sediment pulses are significantly attenuated relative to the coastal sage scrub.

[39] Results from the model also suggest that the grassland hollows will fail more often than coastal sage hollows (Table 2). In the grasslands, the bedrock hollows fill up more rapidly because of higher rates of soil creep and they fail with thinner soil depths because of the weaker root reinforcement. Additionally, the predicted spike in landsliding frequency soon after vegetation conversion (at 10,000 years in Figure 11) is a phenomenon commonly observed

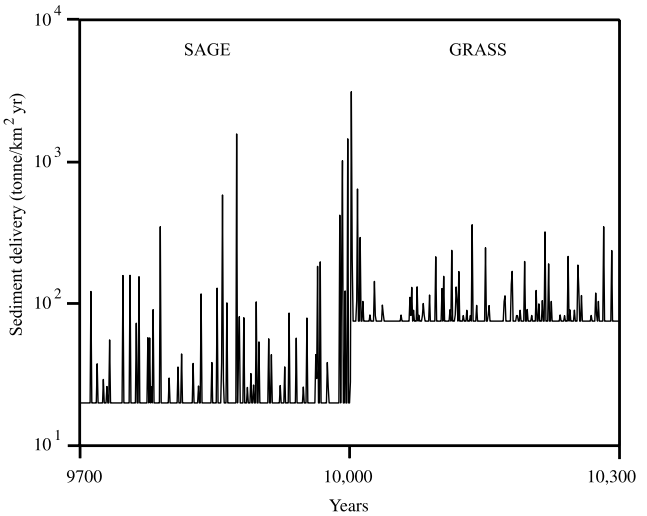

Figure 9. The 600 years bracketing the vegetation conversion. The differences in the magnitude of sediment delivery events between vegetation types are apparent. The flux from soil creep, the baseline sediment delivery, is greater in the grasslands than in the sage, accounting for the higher average rates of sediment loading. Note the semilogarithmic scale.

Table 2. Average Predicted Rates of Sediment Production, Rates of Soil Erosion, and Landslide Frequency[a]

	Production, t km^{-2} yr^{-1}	Erosion, mm kyr^{-1}	Landslides, slides km^{-2} yr^{-1}
Present climate			
Sage scrub	71	60	0.58
Grassland	98	82	1.28
2 × CO_2			
Sage scrub	80	68	0.61
Grassland	100	84	1.55

[a]All differences between vegetation types and climates are statistically significant ($p < 0.005$). The predicted increase in "2 × CO_2" climate scenario is based on results from *Giorgio et al.* [1994] and *Davis and Michaelsen* [1995].

throughout the region [*Corbett and Rice*, 1966; *Bailey and Rice*, 1969; *Rice et al.*, 1969; *Rice and Foggin*, 1971; *Terwilliger and Waldron*, 1991; *Gabet and Dunne*, 2002]. This transient increase in landsliding is likely due to a temporary disequilibrium between the prevailing root reinforcement and soil depths [*Rice and Foggin*, 1971; *Gabet and Dunne*, 2002]. *Gabet and Dunne* [2002] have demonstrated that an abrupt decrease in root reinforcement caused by vegetation conversion increases the likelihood of shallow landsliding on hillslopes that were previously stable.

3.3. Climate Change at Sedgwick Reserve

[40] Given the importance of climate for sediment delivery, it is valuable to consider how global climate change may alter the nature of sediment production. A recently published report has described several potential consequences of global warming in California [*Field et al.*, 1999]. On the basis of general circulation models, the report foresees an increase in winter rains followed by drier summers due to increases in dry, offshore winds (Santa Ana winds). Drier summers would likely increase the frequency and intensity of wildfires throughout the state, particularly in southern California [*Field et al.*, 1999]. *Giorgi et al.* [1994] predicted an approximately 30% increase in winter rainfall and a 4°C rise in summer temperatures in California with a doubling of atmospheric CO_2. Given these estimates, *Davis and Michaelsen* [1995] used an explicit fire ignition

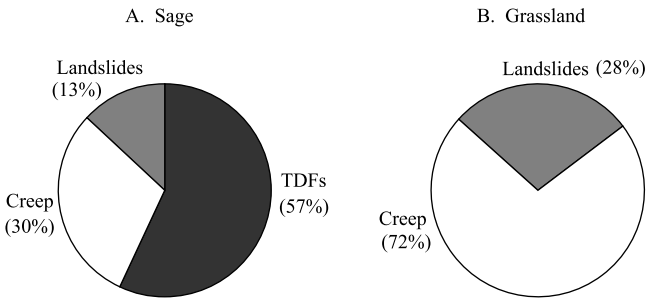

Figure 10. (a) Relative proportions of sediment contributed by each transport process in the sage scrub. The majority of sediment is delivered episodically by TDFs and landslides. (b) Proportions of sediment contributed by each process in the grasslands. The majority of sediment is delivered by soil creep, indicating that sediment delivery in the grasslands tends to occur as a steady trickle rather than as large, infrequent pulses.

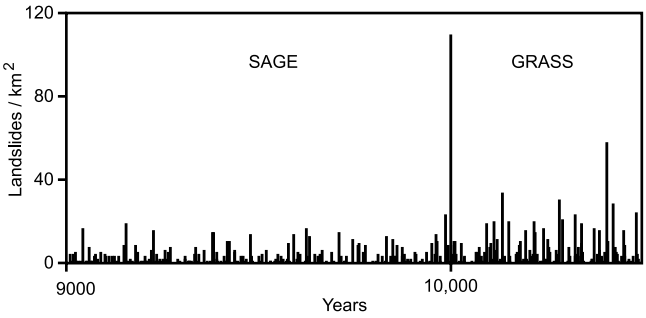

Figure 11. Changes in landslide frequency with vegetation conversion at 10,000 years. Because of the faster rates of hollow-filling and the weaker root reinforcement, landslides occur more frequently in the grasslands. The spike in landslide frequency immediately after the vegetation conversion is a commonly observed phenomenon throughout Mediterranean landscapes and is due to a sudden disequilibrium between soil depths and root reinforcement.

and propagation model to forecast a 17% decrease in the fire recurrence interval in central coastal California.

[41] The model presented here can be used to examine the effects of the predicted changes in the rainfall and fire regimes. First, the annual distribution of rainfall (Figure 4) is shifted to increase the average annual rainfall by 30%, from 50 to 65 cm yr^{-1}. Increased annual rainfall may be accommodated by a rise in the number of storms, storm duration, or rainfall intensity. Climate models suggest that rainfall may become more intense [*Houghton et al.*, 1992] so the average rainfall intensity is increased from 0.18 to 0.23 cm h^{-1}. Second, to account for the change in the fire recurrence interval, the base ignition probability in equation (3) is adjusted to produce a fire recurrence interval of 67 years, instead of 81 years. However, the effect of climate change on the fire recurrence interval is likely more complicated than the simple adjustment made here because the present recurrence interval is largely due to regional fire suppression [*Keeley et al.*, 1999].

[42] The results (Table 2) indicate that climate change will increase the sediment delivery from coastal sage hillslopes by 10% but will only increase the delivery from grassland hillslopes by 2%. This difference would be expected since the sediment delivery processes on sage hillslopes are more sensitive to fires. In both types of vegetation, however, the frequency of landsliding increases due to the more frequent fires that reduce root reinforcement and the larger storms. The increase in storm intensity directly affects the landslide stability analysis through equations (8), (10), and (11) such that the hollows reach a critical saturation more often. The increase in landslide frequency implies that failure volumes will be smaller and that average soil depths in the hollows will decrease [*Gabet and Dunne*, 2002].

[43] On coastal sage hillslopes, the modeled increase in sediment production due to vegetation conversion is nearly 4 times greater than the increase due to climate change. This result leads to the interesting speculation that climatic changes, expressed as purely meteorological phenomena, may only have a minimal impact on changes in sediment production. In contrast, changes in vegetation community driven by regional climate change may have much greater consequences.

4. Conclusion

[44] Sediment loading to channels affects a range of concerns, including debris flow hazards, water quality, and reservoir sedimentation. In this contribution, we present a computer model that drives field-based hillslope sediment transport equations with stochastically generated rainstorms and fires. The model is used to examine how land management strategies and climate change may alter both the rates and the processes of sediment delivery. The results suggest that conversion of coastal sage scrub to grassland, a common practice, increases sediment delivery by approximately 38% but that the sediment delivery regime switches from being dominated by catastrophic processes (e.g., thin debris flows) to being dominated by chronic soil creep processes. The results from the model also suggest that changes in vegetation engendered by changes in climate will increase sediment production more than changes in the climatic events themselves.

[66] **Acknowledgments.** We thank M. Williams, R. Skillins, and V. Boucher of Sedgwick Reserve for their enthusiastic help in facilitating the fieldwork. We are grateful for the help that C. Marcinkovich generously provided in the coding of the model, and we thank the reviewers for their insightful comments. Supplies and salary for E. Gabet were supported by U.C. Water Resources grant UCAL-W-917, NSF-SGER DEB9813669, a Sigma Xi grant, and a Mildred Mathias grant.

References

Anderson, H. W., G. B. Coleman, and P. J. Zinke, Summer slides and winter scour, dry-wet erosion in Southern California mountains, *U.S. For. Serv. Pac. Southwest For. Range Exp. Stn. Tech. Pap., PSW-36*, *PSW-36*, 1959.

Bailey, R. G., and R. M. Rice, Soil slippage: An indicator of slope instability on chaparral watersheds of southern California, *Prof. Geogr.*, *21*(3), 172–177, 1969.

Benda, L., and T. Dunne, Stochastic forcing of sediment routing and storage in channel networks, *Water Resour. Res.*, *33*, 2849–2863, 1997a.

Benda, L., and T. Dunne, Stochastic forcing of sediment supply to channel networks from landsliding and debris flow, *Water Resour. Res.*, *33*, 2865–2880, 1997b.

Beven, K., Towards the use of catchment geomorphology in flood frequency predictions, *Earth Surf. Processes Landforms*, *12*, 69–82, 1987.

Burroughs, E. R., and B. R. Thomas, Declining root strength in Douglas-fir after felling as a factor in slope stability, *USDA For. Serv. Res. Pap.*, *INT-190*, 1977.

Campbell, R. H., Soil slips, debris flows, and rainstorms in the Santa Monica Mountains and vicinity, southern California, *U.S. Geol. Surv. Prof.*, 851, 1975.

Cerda, A., Changes in overland flow and infiltration after a rangeland fire in a Mediterranean scrubland, *Hydrol. Processes*, *12*, 1031–1042, 1998.

Corbett, E. S., and R. M. Rice, Soil slippage increased by brush conversion, *U.S. For. Serv. Pac. Southwest For. Range Exp. Stn. Res. Note*, *PSW-128*, 1–8, 1966.

Davis, F. W., and D. A. Burrows, Modeling fire regime in Mediterranean landscapes, in *Patch Dynamics*, edited by S. Levin, T. Powell, and J. Steele, pp. 247–259, Springer-Verlag, New York, 1993.

Davis, F. W., and J. Michaelsen, Sensitivity of fire regime in chaparral ecosystems to climate change, in *Global Change and Mediterranean-Type Ecosystems*, edited by J. M. Moreno and W. C. Oechel, pp. 435–456, Springer-Verlag, New York, 1995.

Davis, F. W., E. A. Keller, A. Parikh, and J. Florsheim, Recovery of the chaparral riparian zone after wildfire, *USDA For. Serv. Gen. Tech. Rep. PSW-110*, 194–203, 1989.

DeBano, L. F., Water repellent soils: A state of the art, *USDA For. Serv. Res. Pap.*, *PSW-46*, 1–21, 1981.

Denny, C., and J. Goodlett, Microrelief resulting from fallen trees, *U.S. Geol. Surv. Prof. Publ.*, *288*, 59–68, 1956.

Dibblee, T. W. J., Geologic map of the Los Olivos Quadrangle, *Map DF-44*, Dibblee Geol. Found., Santa Barbara, Calif., 1993.

Dietrich, W. E., and T. Dunne, Sediment budget for a small catchment in mountainous terrain, *Z. Geomorphol. Suppl.*, *29*, 191–206, 1978.

Dunne, T., Stochastic aspects of the relations between climate, hydrology and landform evolution, *Trans. Jpn. Geomorphol. Union*, *12*(1), 1–24, 1991.

Eagleson, P. S., Dynamics of flood frequency, *Water Resour. Res.*, *8*(4), 878–898, 1972.

Field, C. B., et al., Confronting climate change in California: Ecological impacts on the Golden State, Union of Concerned Sci. and the Ecol. Soc. of Am., Washington, D. C., 1999.

Fierer, N. G., and E. G. Gabet, Transport of carbon and nitrogen by surface runoff from hillslopes in the Central Coast region of California, *J. Environ. Qual.*, *31*, 1207–1213, 2002.

Florsheim, J. L., E. A. Keller, and D. W. Best, Fluvial sediment transport in response to moderate storm flows following chaparral wildfire, Ventura County, southern California, *Geol. Soc. Am. Bull.*, *103*, 504–511, 1991.

Gabet, E. J., Gopher bioturbation: Field evidence for nonlinear hillslope diffusion, *Earth Surf. Processes Landforms*, *25*(13), 1419–1428, 2000.

Gabet, E. J., Post-fire thin debris flows: Field observations of sediment transport and numerical modeling, *Earth Surf. Processes Landforms*, in press, 2003a.

Gabet, E. J., Sediment transport by dry ravel, *J. Geophys. Res.*, *108*(B1), 2049, doi:10.1029/2001JB001686, 2003b.

Gabet, E. J., and T. Dunne, Landslides on coastal sage-scrub and grassland hillslopes in a severe El Niño winter: The effects of vegetation conversion on sediment delivery, *Geol. Soc. Am. Bull.*, *114*(8), 983–990, 2002.

Gabet, E. J., and T. Dunne, Sediment detachment by rainpower, *Water Resour. Res.*, *39*(1), 1002, doi:10.1029/2001WR000656, 2003.

Gabet, E. J., O. J. Reichman, and E. Seabloom, The effects of bioturbation on soil processes and sediment transport, *Annu. Rev. Earth Planet. Sci.*, *31*, 259–273, 2003.

Giorgi, F., F. S. Brodeur, and G. T. Bates, Regional climate change scenarios over the United States produced with a nested regional climate model, *J. Clim.*, *7*(3), 375–399, 1994.

Hibbert, A. R., Increases in streamflow after converting chaparral to grass, *Water Resour. Res.*, *7*(1), 71–80, 1971.

Horton, J. S., and C. J. Kraebel, Development of vegetation after fire in the chamise chaparral of southern California, *Ecology*, *36*(2), 244–262, 1955.

Houghton, J., B. Callander, and S. Varney (Eds.), Climate change 1992: The supplementary report to the IPCC scientific assessment, 199 pp., Cambridge Univ. Press, New York, 1992.

Iida, T., A stochastic hydro-geomorphological model for shallow landsliding due to rainstorm, *Catena*, *34*, 293–313, 1999.

Keeley, J. A., Resilience of Mediterranean shrub communities to fires, *Ecology*, *45*, 243–245, 1986.

Keeley, J. E., C. J. Fotheringham, and M. Morais, Reexamining fire suppression impacts on brushland fire regimes, *Science*, *284*, 1829–1832, 1999.

Kennett, J. P., and B. L. Ingram, A 20,000-year record of ocean circulation and climate change from the Santa Barbara basin, *Nature*, *377*, 510–514, 1995.

Kirkby, M. J., Hydrological slope models: The influence of climate, in *Geomorphology and Climate*, edited by E. Derbyshire, pp. 247–268, John Wiley, Hoboken, N. J., 1976.

Kirkby, M. J., and I. Statham, Surface stone movement and scree formation, *J. Geol.*, *83*, 349–362, 1974.

Krammes, J. S., Seasonal debris movement from steep mountainside slopes in southern California, in *Proceedings of the Federal Inter-Agency Sedimentation Conference*, *U.S. Dep. of Agric. Misc. Publ. 970*, 85–88, 1965.

Meade, R. H., Factors influencing the early stages of the compaction of clays and sands—Review, *J. Sediment. Petrol.*, *36*(4), 1085–1101, 1966.

Reistenberg, M. M., and S. Sovonick-Dunford, The role of woody vegetation in stabilizing slopes in the Cincinnati area, Ohio, *Geol. Soc. Am. Bull.*, *94*, 506–518, 1983.

Reneau, S. L., and W. E. Dietrich, Erosion rates in the southern Oregon Coast Range: Evidence for an equilibrium between hillslope erosion and sediment yield, *Earth Surf. Processes Landforms*, *16*, 307–322, 1991.

Rice, R. M., Sedimentation in the chaparral: How do you handle unusual events?, in *Sediment Budgets and Routing in Forested Drainage Basins*, edited by F. J. Swanson et al., pp. 39–49, U.S. Dep. of Agric. For. Serv., 1982.

Rice, R. M., and G. T. Foggin, Effect of high intensity storms on soil slippage on mountainous watersheds in southern California, *Water Resour. Res.*, *7*(6), 1485–1496, 1971.

Rice, R. M., E. S. Corbett, and R. G. Bailey, Soil slips related to vegetation, topography, and soil in southern California, *Water Resour. Res.*, *5*(3), 647–659, 1969.

Selby, M. J., *Hillslope Materials and Processes*, Oxford Univ. Press, New York, 1993.

Shipman, G. E., *Soil Survey of Northern Santa Barbara Area, California*, U.S. Dep. of Agric. Soil Conserv. Serv., Washington, D. C., 1972.

Sidle, R. C., A theoretical model of the effects of timber harvesting on slope stability, *Water Resour. Res.*, *28*(7), 1897–1910, 1992.

Sklar, L., and W. E. Dietrich, River longitudinal profiles and bedrock incision models: Stream power and the influence of sediment supply, in *Rivers Over Rock: Fluvial Processes in Bedrock Channels*, *Geophys. Monogr. Ser.*, vol. 107, edited by K. J. Tinkler and E. E. Wohl, pp. 237–260, AGU, Washington, D. C., 1998.

Terwilliger, V. J., and L. J. Waldron, Effects of root reinforcement on soil-slip patterns in the Transverse Ranges of southern California, *Geol. Soc. Am. Bull.*, *103*, 775–785, 1991.

Tucker, G. E., and R. L. Bras, A stochastic approach to modeling the role of rainfall variability in drainage basin evolution, *Water Resour. Res.*, *36*(7), 1953–1964, 2000

Wagner, C. E. V., Age-class distribution and the forest fire cycle, *Can. J. For. Res.*, *8*, 220–227, 1978.

Wells, W. G., The effects of fire on the generation of debris flows in southern California, *Rev. Eng. Geol.*, *7*, 105–114, 1987.

T. Dunne, Donald Bren School of Environmental Science and Management and Department of Geological Sciences, University of California, Santa Barbara, Santa Barbara, CA 93106, USA.

E. J. Gabet, Department of Geology, University of Montana, Missoula, MT 59812, USA. (manny.gabet@mso.umt.edu)